Applied Mathematics and Computation 216 (2010) 395–409

Contents lists available at ScienceDirect

Applied Mathematics and Computation

journal homepage: www.elsevier.com/locate/amc

Numerical modelling of an SIR epidemic model with diffusion

Settapat Chinviriyasit, Wirawan Chinviriyasit *

Department of Mathematics, King Mongkut's University of Technology Thonburi, Bangmod, Thungkru, Bangkok 10140, Thailand

ARTICLE INFO

Keywords:
SIR model
Reaction–diffusion system
Finite-difference method
Whooping cough
Disease-free equilibrium

ABSTRACT

A spatial SIR reaction–diffusion model for the transmission disease such as whooping cough is studied. The behaviour of positive solutions to a reaction–diffusion system with homogeneous Neumann boundary conditions are investigated. Sufficient conditions for the local and global asymptotical stability are given by linearization and by using Lyapunov functional. Our result shows that the disease-free equilibrium is globally asymptotically stable if the contact rate is small. These results are verified numerically by constructing, and then simulating, a robust implicit finite-difference method. Furthermore, the new implicit finite-difference method will be seen to be more competitive (in terms of numerical stability) than the standard finite-difference method.

1. Introduction

Mathematical models for epidemics have been evolving in complexity and realism during the past 60 years. In particular, the study of childhood infections using the SIR (susceptible-infectious-recovered) family of models has yielded many mathematically interesting results [32,25,35,29] and shown good agreement with observations of disease case reports [2,11,12,14,15,19,23,30,33]. An example of this model is the transmission of whooping cough [11,17,18] which is one of the most serious childhood diseases and the cause of more deaths than any other infectious disease apart from measles. According to the different status of a transmitted disease, we denote $S(t), I(t)$ and $R(t)$, respectively, the numbers of individual members who are susceptible, infectious and recovered in the total population size of $N(t)$. Then the SIR model is described by the following system of differential equations [11]:

$$\begin{aligned} \frac{dS}{dt} &= \mu N - \mu S - \beta SI, \\ \frac{dI}{dt} &= -(\mu + v)I + \beta SI, \\ \frac{dR}{dt} &= vI + \mu R. \end{aligned} \tag{1.1}$$

where the parameters μ, v and β denote the death rate (life expectancy = $1/\mu$), the rate of recovery from disease (infectious period = $1/v$) and the transmission coefficient (susceptibility to disease), respectively. It is assumed that the population is mixing thoroughly, so that there is no distinction between individual in one place and those in another. When this is not so, the disease may spread faster in some part than in others and it is necessary to allow the variables to depend on space as well as time.

There is an ongoing interest in the dynamics of infectious diseases and their spatiotemporal spread. Simple compartmental models have been used to understand the principal mechanisms governing disease transmission and have been extended

* Corresponding author.
E-mail address: iwirwong@kmutt.ac.th (W. Chinviriyasit).

0096-3003/$ - see front matter © 2010 Elsevier Inc. All rights reserved.
doi:10.1016/j.amc.2010.01.028

to reaction–diffusion equations to estimate the asymptotic rate of spatial spread [8,9,22]. For diseases with long incubation and infectivity times, the host populations vital dynamics, i.e., birth and death rates, have to be taken into account. This has been shown to qualitatively change the system behaviour. While in the classic Kermack and McKendrick model [20] the disease dies out or becomes endemic if the basic reproductive ratio is less or greater than one, respectively, the infection can also become endemic in models incorporating vital dynamics [5]. If the disease additionally reduces the population size, one has to consider epidemiological models with varying population sizes [7,10,13,37]. This may lead in particular cases to a destabilization of the endemic state and to sustained limit cycle oscillations, as has been numerically observed for the first time by Anderson et al. [1].

It must be pointed out that the system (1.1) neglects any spatial structure of disease spreading and is definitely inapplicable for moving humans individuals. Consequently it is important that the diffusion terms should be taken into consideration in order to investigate whether and how spatial heterogeneity can affect the disease dynamics in (1.1).

In this paper, an SIR reaction–diffusion model, which is an extended version of the SIR epidemic model (1.1), will be studied qualitatively and quantitatively. The aim of this paper is to investigate the asymptotic behaviours of the reaction–diffusion system and to develop numerical method for the solution of an extension model to enable the geographic spread of the disease in a population which has not been vaccinated against it. Let Ω is a bounded domain in R^n with smooth boundary $\partial\Omega$ and η is the outward unit normal vector on the boundary, the SIR reaction–diffusion model can be described by

$$\begin{aligned} &S_t - \alpha\Delta S = \mu N - \mu S - \beta SI, \quad z \in \Omega,\ t > 0,\\ &I_t - \alpha\Delta I = -(\mu + v)I + \beta SI, \quad z \in \Omega,\ t > 0,\\ &R_t - \alpha\Delta I = vI + \mu R, \quad z \in \Omega,\ t > 0, \end{aligned} \tag{1.2}$$

with homogeneous Neumann boundary conditions

$$\partial_\eta S = \partial_\eta I = \partial_\eta R = 0, \quad z \in \partial\Omega,\ t > 0, \tag{1.3}$$

and initial conditions

$$S(z,0) = S_0(z) \geqslant 0, \quad I(z,0) = I_0(z) \geqslant 0, \quad R(z,0) = R_0(z) \geqslant 0, \quad z \in \overline{\Omega}, \tag{1.4}$$

where $S(z,t)$, $I(z,t)$ and $R(z,t)$ denote the numbers of susceptible, infected and recovered individuals at location z and time t. The transmission from susceptibles to infectives is assumed to be βSI where β is the transmissibility coefficient. The spatial propagation of the individuals is modelled by diffusion coefficients $\alpha_S \geqslant 0, \alpha_I \geqslant 0$ and $\alpha_R \geqslant 0$ for the susceptibles, infected and recovered, respectively. Infected individuals are assumed not to be affected by the disease in their mobility, thus $\alpha = \alpha_S = \alpha_I = \alpha_R$. The homogeneous Neumann boundary condition implies that the above system is self-contained and there is no infection across the boundary.

By the maximum principle [28], the populations $S(z,t)$, $I(z,t)$ and $R(z,t)$ are positive for $z \in \overline{\Omega}$ and $t \in (0, T_{max})$, where T_{max} is the maximal existence time for solutions of the system (1.2). Then, both $S(z,t)$, $I(z,t)$ and $R(z,t)$ are bounded on $\overline{\Omega} \times (0, T_{max})$. Hence, it follows from the standard theory for semilinear parabolic systems (see, e.g., [16]) that $T_{max} = \infty$ and so system (1.2) admits a unique classical solution $S(z,t)$, $I(z,t)$ and $R(z,t)$ for all time. As in [3], we define

$$N = \int_\Omega [S(z,0) + I(z,0) + R(z,0)]dz > 0, \quad \text{for all } t > 0, \tag{1.5}$$

to be the total number of individuals in Ω at $t = 0$. We can add three equations in (1.2) and then integrate over Ω to obtain

$$\frac{\partial}{\partial t}\int_\Omega [S + I + R]dz = \int_\Omega \alpha\Delta[S + I + R]dz = 0.$$

This implies that the total population size is a constant, i.e.,

$$\int_\Omega [S + I + R]dz = N, \quad \text{for all } t \geqslant 0. \tag{1.6}$$

Throughout this paper, the total population, N, is a fixed positive constant then system (1.2) can reduce to a one of two equations,

$$\begin{aligned} &S_t - \alpha\Delta S = \mu N - \mu S - \beta SI,\\ &I_t - \alpha\Delta I = -(\mu + v)I + \beta SI, \end{aligned} \tag{1.7}$$

and determining R from $R(z,t) = N - S(z,t) - I(z,t)$ or

$$R_t - \alpha\Delta I = vI + \mu R, \quad z \in \Omega, t > 0. \tag{1.8}$$

This paper is organized as follows. The uniform bounds for the solutions of (1.7) are given in Section 2. In Section 3, local and global stabilities of the equilibria are discussed and deals with asymptotical behaviours of the solutions to the system (1.7). A competitive implicit finite-difference method for the solution of the system {(1.7), (1.3), (1.4)} is constructed in Section 4. Numerical experiments are reported in Section 5.

2. Uniform bound

Since the initial values are positive and the growth functions in the right hand of (1.7) are assumed to be sufficiently smooth in R^2_+, standard partial differential equations (PDEs) theory shows that the solutions of (1.7) are unique and continuous for all positive time in Ω. The following results show that the solutions of (1.7) is positive and uniformly bounded. We first present a positivity lemma, which can be found in any standard textbook on PDEs.

Lemma 2.1. *Suppose* $w \in C(\overline{\Omega} \times [0,\tau]) \bigcap C^{2,1}(\Omega \times (0,\tau])$ *and satisfies*

$$\begin{aligned} &w_t - D\Delta w \geqslant c(z,t)w, && x \in \Omega,\ 0 < t \leqslant \tau, \\ &\frac{\partial w}{\partial \eta} \geqslant 0, && x \in \partial\Omega,\ 0 < t \leqslant \tau, \\ &w(z,0) \geqslant 0, && x \in \overline{\Omega}, \end{aligned} \tag{2.1}$$

where $c(z,t) \in C(\overline{\Omega} \times [0,\tau])$. *Then* $w(z,t) \geqslant 0$ *on* $\overline{\Omega} \times [0,\tau]$. *Moreover,* $w(z,t) > 0$ *or* $w \equiv 0$ *in* $\Omega \times [0,\tau]$.

As a consequence of Lemma 2.1, we have the following positivity result.

Lemma 2.2. *Any solution of (1.7) with a positive initial function is positive.*

Proof. Let (S,I) be a solution of (1.7) in $\Omega \times [0,T_{max})$. Then for any τ with $0 < \tau < T_{max}$, direct using Lemma 2.1 to the second equation of (1.7) becomes

$$I_t - \alpha\Delta I = b_{22}I, \quad z \in \Omega,\ 0 < t \leqslant \tau, \tag{2.2}$$

where $b_{22} = -(\mu + v) + \beta S$. Since b_{22} is bounded in $\Omega \times [0,\tau]$, it follows form Lemma 2.1 that $I > 0$ in $\Omega \times (0,\tau]$. Similarly we have $S > 0$ in $\Omega \times (0,\tau]$ since that

$$S_t - \alpha\Delta S \geqslant -(\mu + \beta I)S, \quad z \in \Omega,\ 0 < t \leqslant \tau. \tag{2.3}$$

As τ is arbitrary in $(0,T_{max})$, we have $S > 0$ and $I > 0$ in $\Omega \times [0,T_{max})$. □

Theorem 2.1. *Let* $(S,I) \in \left[C(\overline{\Omega} \times [0,T_{max})) \bigcap C^{2,1}(\Omega \times (0,T_{max}))\right]^2$ *be the solution of (1.7) with non-negative non-trivial initial values. Then* $T = \infty$ *and*

$$0 < S(z,t) + I(z,t) \leqslant max\{\|S_0(z) + I_0(z)\|_\infty, N\}.$$

Proof. We show that $S(z,t)$ and $I(z,t)$ are bounded from above on $\Omega \times [0,T_{max})$. Since $0 < S(z,0) + I(z,0) \leqslant \|S_0(z) + I_0(z)\|_\infty$ and $(S+I)_t - \alpha\Delta(S+I) \leqslant \mu N - \mu(S+I)$, we have that $0 < S(z,t) + I(z,t) \leqslant W(t)$ for $(z,t) \in \Omega \times [0,T_{max})$, where $W(t) = [N + (\|(S_0(z) + I_0(z)\|_\infty - N)e^{-\mu t}]$ for $t \in [0,\infty)$ is the solution of the problem

$$\frac{dW(t)}{dt} = \mu N - \mu W(t), \quad W(0) = \|S_0(z) + I_0(z)\|_\infty.$$

Hence we have $0 < W(t) < max\{\|S_0(z) + I_0(z)\|_\infty, N\}$ for $t \in [0,\infty)$ and thus $0 < S(z,t) + I(z,t) \leqslant W(z) \leqslant max\{\|S_0(z) + I_0(z)\|_\infty, N\}$. □

3. Qualitative analysis

In this section, the local and global stabilities of the positive stationary solution for (1.7) is discussed. It is clear that the system (1.7) always has the disease-free equilibrium $e^0 = (N,0)$, which represents that no infected individual exists. Further, if the following conditions are satisfied

$$r_0 = \frac{N\beta}{\mu + v}, \tag{3.1}$$

then the system (1.7) also has an endemic equilibrium $e^* = (S^*, I^*)$, where $S^* = \frac{\mu N}{\mu + v}$ and $I^* = \frac{\mu N}{\mu + v} - \frac{\mu}{\beta}$. In epidemic terms, this implies that there exists an epidemic equilibrium provided that the contact rate β of the infected is big. Following the standard technique as in [26], let $\mu_1 < \mu_2 < \mu_3 < \cdots$ be the eigenvalues of the operator $-\Delta$ on Ω with the homogeneous Neumann boundary condition. Let $\mathbf{V} = \{\mathbf{u} = (S,I) \in [C(\overline{\Omega})]^2 | \partial_\eta S = \partial_\eta I = 0 \text{ on } \partial\Omega\}$ and $\mathbf{V}_i$ be the invariant subspace of $\mathbf{V}$ for a given eigenvalue μ_i so that $\oplus_{i=1}^{\infty}\mathbf{V}_i$.

Let

$$L = \begin{pmatrix} \alpha\Delta & 0 \\ 0 & \alpha\Delta \end{pmatrix} + \begin{pmatrix} -\mu - \beta I^* & -\beta S^* \\ \beta I^* & \beta S^* - (\mu + v) \end{pmatrix}.$$

Then the linearization of the system (1.7) is $\mathbf{u}_t = L\mathbf{u}$, and since $\mathbf{V}_i$ is invariant under the operator L for each $i \geqslant 1, \lambda$ is an eigenvalue of L on $\mathbf{V}_i$ if and only if it is an eigenvalue of the matrix

$$L = \begin{pmatrix} -\alpha\mu_i & 0 \\ 0 & -\alpha\mu_i \end{pmatrix} + \begin{pmatrix} -\mu - \beta I^* & -\beta S^* \\ \beta I^* & \beta S^* - (\mu + \nu) \end{pmatrix}.$$

The characteristic equation is given by

$$\varphi_i(\lambda) \triangleq (\lambda + \mu_i\alpha + \mu + \beta I^*)(\lambda + \mu_i\alpha + \mu + \nu - \beta S^*) - \beta^2 S^* I^* = 0.$$

First, we consider the disease-free equilibrium e^0. The eigenvalues are $-\mu_i\alpha - \mu$ and $-\mu_i\alpha - \mu - \nu$. If $r_0 > 1$, there is a positive eigenvalue $\beta N - \mu(\mu + \nu)$ and then e^0 is unstable while if $r_0 < 1, e^0$ is locally asymptotically stable since that all eigenvalues are less than a negative constant.

As for the equilibrium e^*, the characteristic equation is

$$\varphi_i(\lambda) = (\lambda + \mu_i\alpha)^2 + A(\lambda + \mu_i\alpha) + B = 0,$$

where

$$A = 2\mu + \nu + \beta(I^* - S^*),$$
$$B = \mu(\mu + \nu) + \mu\beta(I^* - S^*) + \nu\beta I^*.$$

If $r_0 > 1$, we have $A > 0$ and $B > 0$, therefore all roots of the characteristic equation have negative real parts. It follows from Theorem 5.1.1 of [16] that e^* is locally asymptotically stable. In summary, we have proved the following theorem.

Theorem 3.1. *If $r_0 > 1$, then the endemic equilibrium is locally asymptotically stable and the disease-free equilibrium is unstable. On the contrary, if $r_0 < 1$, then the disease-free equilibrium is locally asymptotically stable.*

Next, we consider the global stability of the system (1.7). Define

$$V(t) = \int_\Omega \frac{1}{2}(S - N)^2 dz + N\int_\Omega I dz. \tag{3.2}$$

Calculating the derivative of $V(t)$ along the positive solution of the system (1.7) yields

$$\frac{dV(t)}{dt} = -\alpha\int_\Omega \Big(|\nabla S|^2 + N|\nabla I|^2\Big)dz - \int_\Omega \Big((\mu + \beta I)(S - N)^2 + N(\mu + \nu)(1 - r_0)I\Big)dz, \tag{3.3}$$

when $r_0 < 1, \frac{dV(t)}{dt} \leqslant 0$. Moreover, it follows from Lemma 2.1 in [21] that

$$\lim_{t\to\infty}\int_\Omega \Big[|\nabla S|^2 + |\nabla I|^2 + (S(z,t) - N)^2 + (I(z,t) - 0)^2\Big]dz = 0. \tag{3.4}$$

Applying the Poincaré inequality

$$\int_\Omega \mu_2|S - \bar{S}|^2 dz \leqslant \int_\Omega |\nabla S|^2 dz, \quad \int_\Omega \mu_2|I - \bar{I}|^2 dz \leqslant \int_\Omega |\nabla I|^2 dz,$$

yields

$$\lim_{t\to\infty}\int_\Omega [(S - \bar{S})^2 + (I - \bar{I})^2]dz = 0, \tag{3.5}$$

where $\bar{S}(t) = \frac{1}{|\Omega|}\int_\Omega S(x,t)dz$ is the smallest positive eigenvalue of operator Laplace with homogeneous Neumann condition. Hence,

$$|\Omega|(\bar{S} - N)^2 = \int_\Omega (\bar{S} - N)^2 dz = \int_\Omega \Big(\bar{S}(t) - S(z,t) + S(z,t) - N\Big)^2 dz \leqslant 2\int_\Omega \Big(\bar{S}(t) - S(z,t)\Big)^2 dz + 2\int_\Omega (S(z,t) - N)^2 dz.$$

So we have $\bar{S}(t) \to N$ as $t \to \infty$. Similarly, $\bar{I}(t) \to 0$ as $t \to \infty$.

Noticing that the solution of the system (1.7) is bounded, there exist a subsequence $\{t_m\}$, and non-negative functions $W_1, W_2 \in C^2(\overline{\Omega})$, such that

$$\lim_{m\to\infty}\|S(\cdot,t_m) - W_1(\cdot)\|_{C^2(\overline{\Omega})} = 0, \quad \lim_{m\to\infty}\|I(\cdot,t_m) - W_2(\cdot)\|_{C^2(\overline{\Omega})} = 0.$$

Applying (3.5), and noting that, in fact, $\bar{S} \to N$ and $\bar{I} \to 0$, we have $W_1 \equiv N$ and $W_2 \equiv 0$. Therefore,

$$\lim_{m\to\infty}\|S(\cdot,t_m) - N\|_{C^2(\overline{\Omega})} = 0, \quad \lim_{m\to\infty}\|I(\cdot,t_m) - 0)\|_{C^2(\overline{\Omega})} = 0,$$

which combining with the local stability gives the global stability of e^0.

For the endemic equilibrium e^*, we define

$$V(t) = \int_\Omega \left(S - S^* - S^*\log\frac{S}{S^*}\right)dz + \int_\Omega \left(I - I^* - I^*\log\frac{I}{I^*}\right)dz. \tag{3.6}$$

Direct calculating the derivative of $V(t)$ yields

$$\frac{dV(t)}{dt} = \int_\Omega \left[S_t\left(1-\frac{S^*}{S}\right) + I_t\left(1-\frac{I^*}{I}\right)\right]dz = -\alpha\int_\Omega \left[S^*\frac{|\nabla S|^2}{S^2} + I^*\frac{|\nabla I|^2}{I^2}\right]dz - \frac{\mu N\beta}{\mu+\nu}\int_\Omega \frac{(S-S^*)^2}{S}dz \leqslant 0.$$

Similarly, we have the following stability result:

Theorem 3.2. *If $r_0 < 1$, then the disease-free equilibrium e^0 is globally asymptotically stable. On the other hand, if $r_0 > 1$, then the endemic equilibrium e^* with non-trivial initial functions is globally asymptotically stable.*

4. Numerical methods

In this section, we rewrite the equations in (1.7) as (see also [27]):

$$\frac{\partial S}{\partial t} = \mu N - \mu S - \beta SI + \alpha\frac{\partial^2 S}{\partial z^2}, \tag{4.1}$$

$$\frac{\partial I}{\partial t} = -(\mu+\nu)I + \beta SI + \alpha\frac{\partial^2 I}{\partial z^2}, \tag{4.2}$$

for all $t \geqslant 0, z \in [0, L]$. The initial conditions are of the form

$$S(z,0) = S_0, \quad I(z,0) = I_0; \quad 0 \leqslant z \leqslant L, \tag{4.3}$$

and the boundary conditions are

$$\frac{\partial S(0,t)}{\partial z} = \frac{\partial I(0,t)}{\partial z} = 0; \quad t > 0, \tag{4.4}$$

$$\frac{\partial S(L,t)}{\partial z} = \frac{\partial I(L,t)}{\partial z} = 0; \quad t > 0. \tag{4.5}$$

4.1. Discretization and notations

A solution of the system of partial differential equations (4.1)–(4.5) may be computed by finite-difference methods by discretizing the space interval $[0, L]$ into M sub-intervals each of width $h > 0$, and the time interval $t \geqslant 0$ is discretized in steps each of length $\ell > 0$. The open region $\Omega = [0, L] \times [t > 0]$ and its boundary $\partial\Omega$ consisting of the lines $z = 0, z = L$ and $t = 0$ are thus covered by a rectangular mesh, the mesh points having coordinates of the form $(z_m, t_n) = (mh, n\ell)$ where $z_m = mh (m = 0, 1, 2, \ldots, M)$ and $t_n = n\ell (n = 0, 1, 2, \ldots)$.

The solutions of (4.1)–(4.5) at the typical mesh point (z_m, t_n) are, of course, $S(z_m, t_n)$ and $I(z_m, t_n)$ which will be denoted by S_m^n and I_m^n, respectively. The theoretical solution of an approximating finite-difference method for (4.1) and (4.2) at the same mesh point (z_m, t_n) will be denoted by X_m^n and Y_m^n, respectively, while the values actually obtained, which may be subject, for example, to round-off errors, will be denoted by $\widetilde{X}_m^n$ and $\widetilde{Y}_m^n$, respectively.

A family of numerical methods will be developed by approximating the time derivatives in (4.1) and (4.2) by the first-order forward-difference replacement

$$\frac{\partial u(z,t)}{\partial t} = \frac{u(z,t+\ell) - u(z,t)}{\ell} + O(\ell) \quad \text{as } \ell \to 0, \tag{4.6}$$

and the space derivatives in (4.1) and (4.2) by the weighted approximant

$$\frac{\partial^2 u(z,t)}{\partial z^2} \approx h^{-2}[\theta\{u(z-h,t+\ell) - 2u(z,t+\ell) + u(z+h,t+\ell)\} + (1-\theta)\{u(z-h,t) - 2u(z,t) + u(z+h,t)\}], \tag{4.7}$$

in which $u(z,t)$ represents $S(z,t)$ or $I(z,t)$ and $0 \leqslant \theta \leqslant 1$ is a parameter. When $\theta = 0$, (4.7) is $O(h^2)$ as $h, \ell \to 0$ and is $O(h^2 + \ell)$ as $h, \ell \to 0$ otherwise.

4.2. Development of finite-difference method

A competitive finite-difference method for solving S in (4.1), based on approximating the time derivative in (4.6) and the space derivative in (4.7) and making appropriate approximations for the right hand side, is

$$\frac{X_m^{n+1} - X_m^n}{\ell} = \mu N - \mu X_m^{n+1} - \beta X_m^{n+1} Y_m^n + \alpha\theta\frac{X_{m-1}^{n+1} - 2X_m^{n+1} + X_{m+1}^{n+1}}{h^2} + \alpha(1-\theta)\frac{X_{m-1}^n - 2X_m^n + X_{m+1}^n}{h^2}. \tag{4.8}$$

Similarly, the method for I given by

$$\frac{Y_m^{n+1} - Y_m^n}{\ell} = -(\mu+\nu)Y_m^{n+1} + \beta X_m^n Y_m^n + \alpha\theta\frac{Y_{m-1}^{n+1} - 2Y_m^{n+1} + Y_{m+1}^{n+1}}{h^2} + \alpha(1-\theta)\frac{Y_{m-1}^n - 2Y_m^n + Y_{m+1}^n}{h^2}. \tag{4.9}$$

Eqs. (4.8) and (4.9) may be re-arranged to give

$$-p\theta X_{m-1}^{n+1}+(1+\mu\ell+\ell\beta Y_m^n+2p\theta)X_m^{n+1}-p\theta X_{m+1}^{n+1}=p(1-\theta)X_{m-1}^n+\{1-2p(1-\theta)\}X_m^n+p(1-\theta)X_{m+1}^n+\ell\mu N, \tag{4.10}$$

and

$$-p\theta Y_{m-1}^{n+1}+(1+(\mu+\nu)\ell+2p\theta)Y_m^{n+1}-p\theta Y_{m+1}^{n+1}=p(1-\theta)Y_{m-1}^n+\{1+\ell\beta X_m^n-2p(1-\theta)\}Y_m^n+p(1-\theta)Y_{m+1}^n, \tag{4.11}$$

where $p=\alpha\ell/h^2, m=0,1,2,\ldots,M$ and $n=0,1,2,\ldots$. This method {(4.10) and (4.11)} is denoted as method $DM(\theta)$. Verification of accuracy may be obtained by considering the local truncation error associated with {(4.10) and (4.11)} at the point $(x,t)=(x_m,t_n)$ may be obtained from {(4.8) and (4.9)} and given by

$$\begin{aligned}\mathscr{L}_S[S(z,t),I(z,t):h,\ell]&=\ell^{-1}[S(z,t+\ell)-S(z,t)]-\mu N+\{\mu+\beta I(z,t)\}S(z,t+\ell)\\&\quad-\alpha\theta h^{-2}\{S(z-h,t+\ell)-2S(z,t+\ell)+S(z+h,t+\ell)\}\\&\quad-(1-\theta)\alpha h^{-2}\{S(z-h,t)-2S(z,t)+S(z+h,t)\}\\&\quad-\left[\frac{\partial S}{\partial t}-\mu N+\{\mu+\beta I(z,t)\}S(z,t)-\alpha\frac{\partial^2 S}{\partial z^2}\right],\end{aligned} \tag{4.12}$$

$$\begin{aligned}\mathscr{L}_I[S(z,t),I(z,t):h,\ell]&=\ell^{-1}[I(z,t+\ell)-I(z,t)]+(\mu+\nu)I(z,t+\ell)-\beta S(z,t)I(z,t)\\&\quad-\alpha\theta h^{-2}\{I(z-h,t+\ell)-2I(z,t+\ell)+I(z+h,t+\ell)\}\\&\quad-(1-\theta)\alpha h^{-2}\{I(z-h,t)-2I(z,t)+I(z+h,t)\}\\&\quad-\left[\frac{\partial I}{\partial t}+\{(\mu+\nu)-\beta S(z,t)\}I(z,t)-\alpha\frac{\partial^2 I}{\partial z^2}\right].\end{aligned} \tag{4.13}$$

Expanding $S(z,t+\ell), S(z\pm h,t+\ell), S(z\pm h,t), I(z,t+\ell), I(z\pm h,t+\ell)$ and $I(z\pm h,t)$ in (4.12) and (4.13) as Taylor series about (x,t) lead to

$$\mathscr{L}_S[S(z,t),I(z,t);h,\ell]=-\frac{1}{12}\alpha h^2\frac{\partial^4 S}{\partial z^4}+\ell\left[\frac{1}{2}\frac{\partial^2 S}{\partial t^2}+\mu\frac{\partial S}{\partial t}+\beta I\frac{\partial S}{\partial t}-\alpha\theta\frac{\partial^3 S}{\partial z^2\partial t}\right]+\cdots, \tag{4.14}$$

$$\mathscr{L}_I[S(z,t),I(z,t);h,\ell]=-\frac{1}{12}\alpha h^2\frac{\partial^4 I}{\partial z^4}+\ell\left[\frac{1}{2}\frac{\partial^2 I}{\partial t^2}+(\mu+\nu)\frac{\partial I}{\partial t}-\alpha\theta\frac{\partial^3 I}{\partial z^2\partial t}\right]+\cdots. \tag{4.15}$$

Eqs. (4.14) and (4.15) verify that method $DM(\theta)$ is $O(h^2+\ell)$ as $h,\ell\to 0$.

4.3. Standard finite-difference method

The corresponding standard finite-difference method for solving the initial/boundary value problems (IBVP) (see [36]), obtained by using (4.6) and (4.7) in (4.1) and (4.2) and evaluating the right-hand functions in (4.1) and (4.2) at base time level $t=t_n$, is given by, respectively,

$$\frac{X_m^{n+1}-X_m^n}{\ell}=\mu N-\mu X_m^n-\beta X_m^n Y_m^n+\theta\,\frac{X_{m-1}^{n+1}-2X_m^{n+1}+X_{m+1}^{n+1}}{h^2}+(1-\theta)\,\frac{X_{m-1}^n-2X_m^n+X_{m+1}^n}{h^2}, \tag{4.16}$$

and

$$\frac{Y_m^{n+1}-Y_m^n}{\ell}=-(\mu+\nu)Y_m^n+\beta X_m^n Y_m^n+\theta\,\frac{Y_{m-1}^{n+1}-2Y_m^{n+1}+Y_{m+1}^{n+1}}{h^2}+(1-\theta)\,\frac{Y_{m-1}^n-2Y_m^n+Y_{m+1}^n}{h^2}. \tag{4.17}$$

After rearranging, Eqs. (4.16) and (4.17) become

$$-p\theta X_{m-1}^{n+1}+(1+2p\theta)X_m^{n+1}-p\theta X_{m+1}^{n+1}=p(1-\theta)X_{m-1}^n+\{1-\ell\mu-\ell\beta Y_m^n-2p(1-\theta)\}X_m^n+p(1-\theta)X_{m+1}^n+\ell\mu N, \tag{4.18}$$

$$-p\theta Y_{m-1}^{n+1}+(1+2p\theta)Y_m^{n+1}-p\theta Y_{m+1}^{n+1}=p(1-\theta)Y_{m-1}^n+\{1-(\mu+\nu)\ell+\ell\beta X_m^n-2p(1-\theta)\}Y_m^n+p(1-\theta)Y_{m+1}^n, \tag{4.19}$$

where $p=\alpha\ell/h^2, m=0,1,2,\ldots,M$ and $n=0,1,2,\ldots$. This method {(4.18) and (4.19)} is denoted as method $SM(\theta)$. The local truncation error associated with {(4.18) and (4.19)} at the point $(x,t)=(x_m,t_n)$ may be obtained from {(4.16) and (4.17)}. Using Taylor series expansion, the associated local truncation errors of the method $SM(\theta)$ are, respective,

$$\mathscr{L}_S[S(z,t),I(z,t);h,\ell]=-\frac{1}{12}\alpha h^2\frac{\partial^4 S}{\partial z^4}+\ell\left[\frac{1}{2}\frac{\partial^2 S}{\partial t^2}-\alpha\theta\frac{\partial^3 S}{\partial z^2\partial t}\right]+\cdots, \tag{4.20}$$

$$\text{and }\mathscr{L}_I[S(z,t),I(z,t);h,\ell]=-\frac{1}{12}\alpha h^2\frac{\partial^4 I}{\partial z^4}+\ell\left[\frac{1}{2}\frac{\partial^2 I}{\partial t^2}-\alpha\theta\frac{\partial^3 I}{\partial z^2\partial t}\right]+\cdots. \tag{4.21}$$

Eqs. (4.20) and (4.21) verify that method $SM(\theta)$ is $O(h^2+\ell)$ as $h, \ell \to 0$. The proof of the stabilities and implementations of the methods $SM(\theta)$ and $DM(\theta)$ are given in the Appendix A and B, respectively.

5. Numerical experiments

5.1. Experiment 1: Effect of time-step, ℓ

In order to test the stability and convergence properties of the novel scheme constructed in Section 4, we use the methods $DM(\theta)$ and $SM(\theta)$ to simulate the model (4.1)–(4.3) with the following set of biologically feasible parameter values (see [11]): $\mu = 0.04\ \text{year}^{-1}, \nu = 24\ \text{year}^{-1}, N = 3\times 10^5$ and the infection rate, β, chosen to be $\beta = 4.4333\times 10^{-4}$. The values of μ and ν refer to an average life expectancy of 25 years and an infectious period of 15 days (approximately). Furthermore, the following initial subpopulation sizes were chosen for simulation purposes:

$$S(z_i,0) = \begin{cases} 325000z, & 0 \leqslant z < 0.5, \\ -325000(z-1) & 0.5 \leqslant z \leqslant 1, \end{cases}$$

$$I(z_i,0) = \begin{cases} 7500z & 0 \leqslant z < 0.5, \\ -7500(z-1) & 0.5 \leqslant z \leqslant 1. \end{cases}$$

Fig. 1 shows the maximum value of each class of individuals is concentrated at the middle of the interval $0 \leqslant z \leqslant 1$ and the numbers decrease linearly to zero at the boundaries $z = 0$ and $z = 1$.

The effect of the time-step on the methods $SM(\theta)$ and $DM(\theta)$ with $\theta = 0, \frac{1}{2}, 1$ was monitored for the different values of the diffusion rate, α. The numerical results are obtained using $\alpha = 0.001, 0.01, 0.04$ and the stability intervals of the numerical

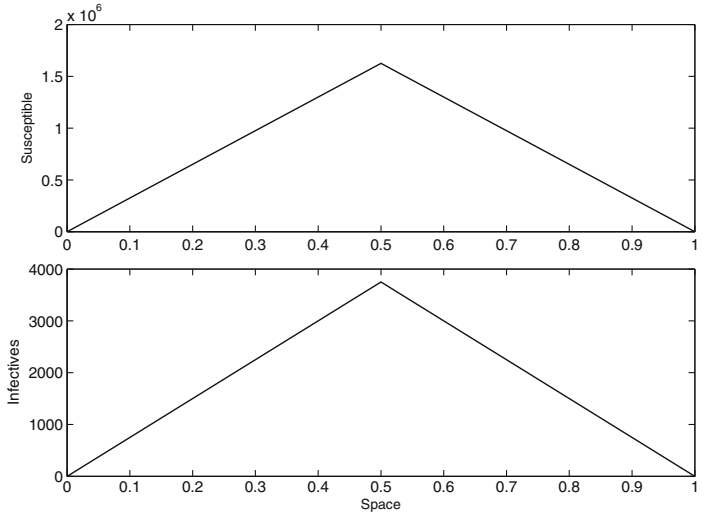

Fig. 1. The initial distributions of the numbers of susceptibles and infectious individuals for Experiments 1 and 2.

Table 1
Stability intervals of the methods.

α	θ	Interval of stability	
		Method $SM(\theta)$	Method $DM(\theta)$
0.001	0	(0, 0.0334)	(0, 0.3250)
	$\frac{1}{2}$	(0, 0.0334)	∞
	1	(0, 0.0280)	∞
0.01	0	(0, 0.0245)	(0, 0.0311)
	$\frac{1}{2}$	(0, 0.0326)	(0, 3.0000)
	1	(0, 0.0317)	∞
0.04	0	(0, 0.0065)	(0, 0.0076)
	$\frac{1}{2}$	(0, 0.0340)	∞
	1	(0, 0.0445)	(0, 0.2000)

methods are tabulated in Table 1. In the case method $SM(\theta)$ with $\theta = 0$ negative values of susceptible individuals, S, and infectious individuals, I, occurred for $\ell > 0.0334$ with $\alpha = 0.001$ while contrived oscillations were exhibited in the numerical solution as ℓ was increased beyond the value 0.0245 with $\alpha = 0.01$ and the value 0.0065 with $\alpha = 0.04$. The method produced overflow for $\ell > 0.0467$ with $\alpha = 0.001$, for $\ell > 0.0257$ with $\alpha = 0.01$ and for $\ell > 0.0077$ with $\alpha = 0.04$. Using $\theta = \frac{1}{2}$ and $\theta = 1$ negative values of susceptible and infectious individuals began as ℓ was increased above the values in the stability interval (see Table 1) with overflow occurring as ℓ was increased further.

Using method $DM(\theta)$ with $\theta = 0$ oscillations occurred for $\ell > 0.3250$ with $\alpha = 0.001$, for $\ell > 0.0311$ with $\alpha = 0.01$ and for $\ell > 0.0076$ with $\alpha = 0.04$ with overflow occurring for $\ell > 0.3399(\alpha = 0.001)$, for $\ell > 0.0329(\alpha = 0.01)$ and for $\ell > 0.0083(\alpha = 0.04)$. Using $\theta = \frac{1}{2}$ with $\alpha = 0.001$ the method never produced overflow and always gave the qualitatively correct behaviour for all $\ell > 0$ whereas with $\alpha = 0.01$ the method did not produced overflow but the qualitatively correct behaviour was observed for rather time step values of ℓ, see Table 1. For $\alpha = 0.04$ the oscillations began for $\ell > 0.2000$ with overflow occurring for $\ell > 17.5876$. Using $\theta = 1$ with $\alpha = 0.001, 0.01, 0.04$ the qualitatively correct behaviour was observed for an arbitrarily large time step ℓ.

As above described and Table 1, it is verified that method $DM(\theta)$ has a much better stability property than method $SM(\theta)$.

The method $DM(\theta)$ with $\theta = 1$ will now be used to simulate the model to monitor the effects of the diffusive rate (see Experiment 2) and the transmissibility coefficient (see Experiment 3).

5.2. Experiment 2: Effect of diffusive rate, α

To monitor the effect of diffusive rate, we simulate the model using the method $DM(\theta), \theta = 1$ with the same parameters and initial conditions as in Experiment 1. The space and time steps were given the value $h = 0.025, \ell = 0.001$ and the

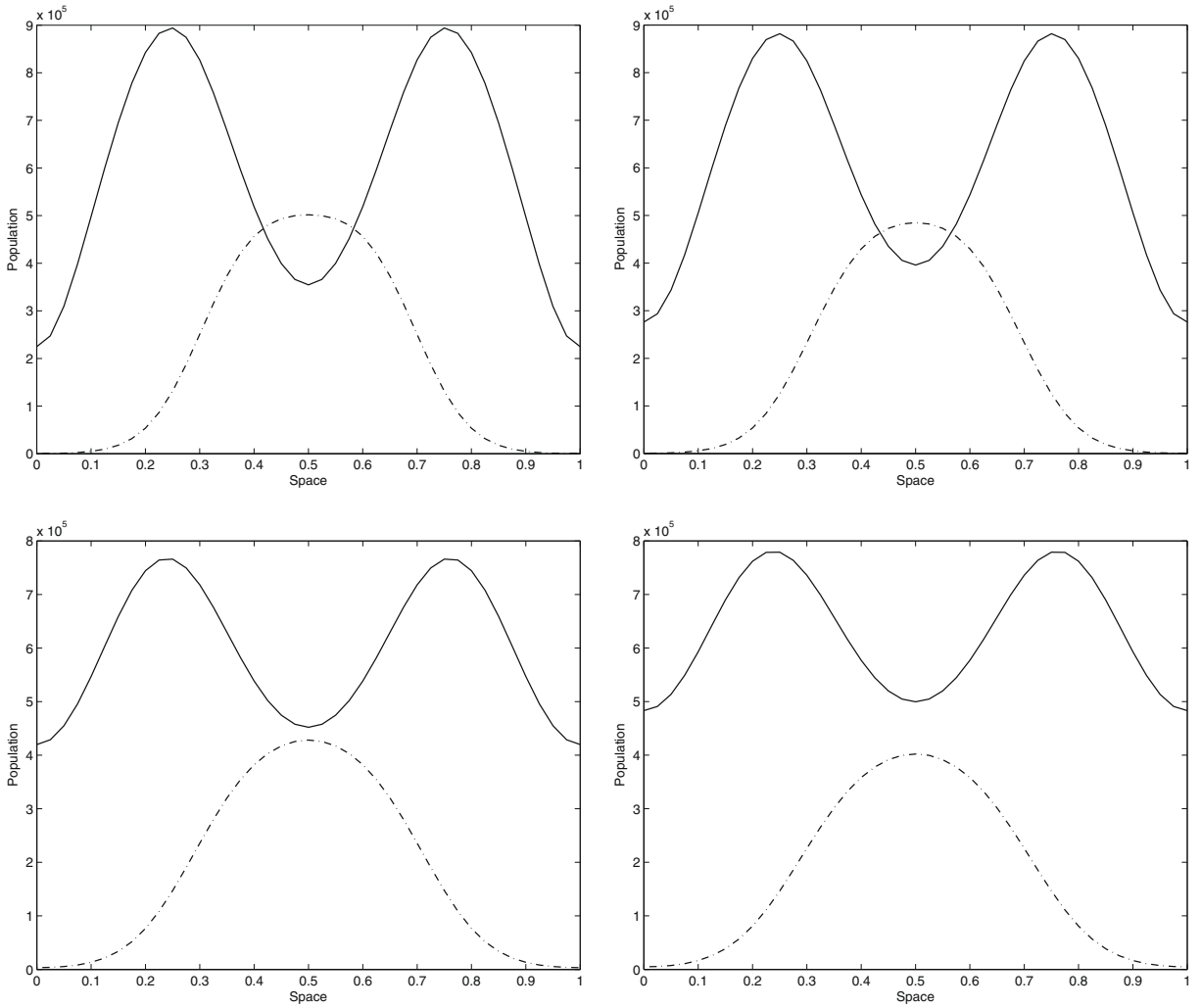

Fig. 2. Numerical simulation of the model (1.2) at time $t = 0.1$ with $h = 0.025, \ell = 0.001$ and $r_0 = 5.53$; susceptible individual $(-)$ and infectious individual $(-)$; (a) $\alpha = 0.0005$, (b) $\alpha = 0.001$, (c) $\alpha = 0.01$, (d) $\alpha = 0.04$.

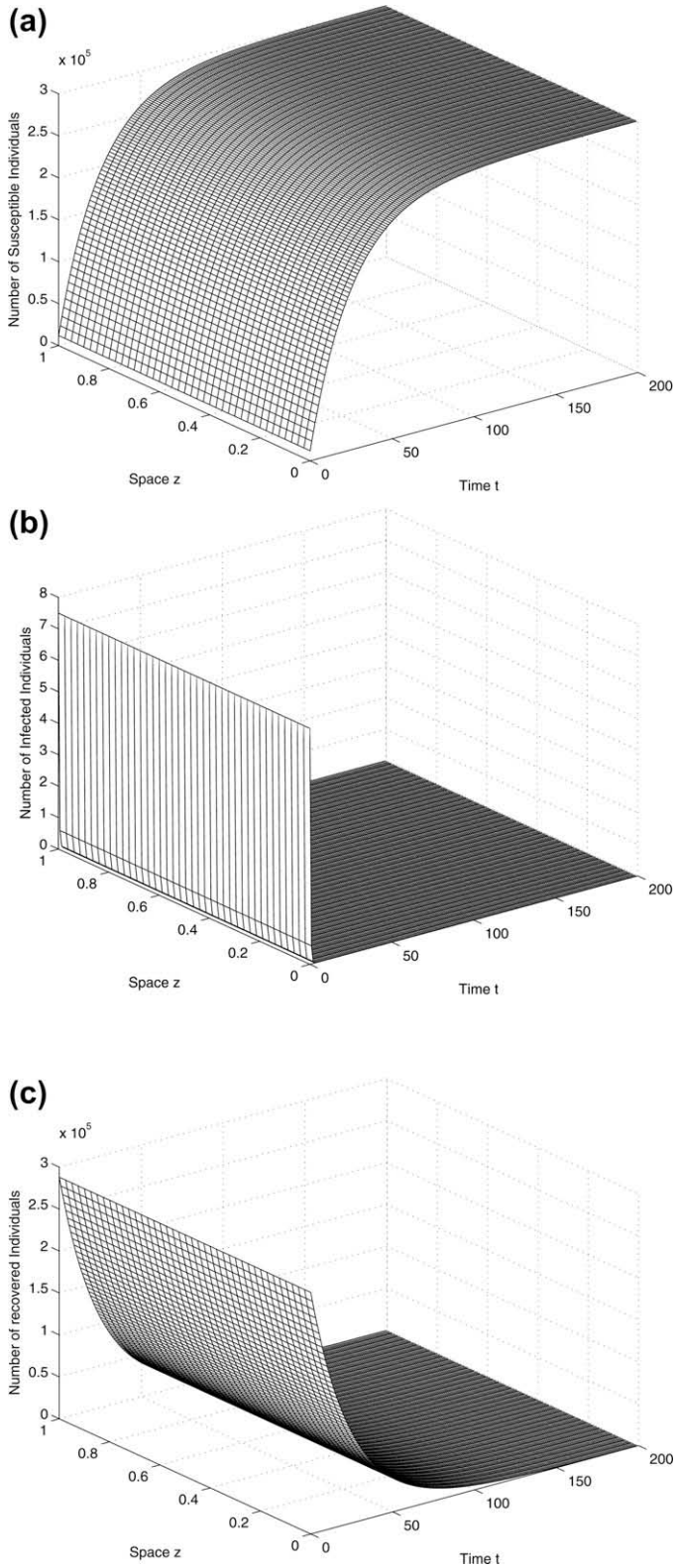

Fig. 3. Numerical simulation of the model (1.2) with $h = 0.025, \ell = 0.5$ and $r_0 = 0.9567$: (a) profiles for susceptibles, (b) profiles for infectives and (c) profiles for recovered.

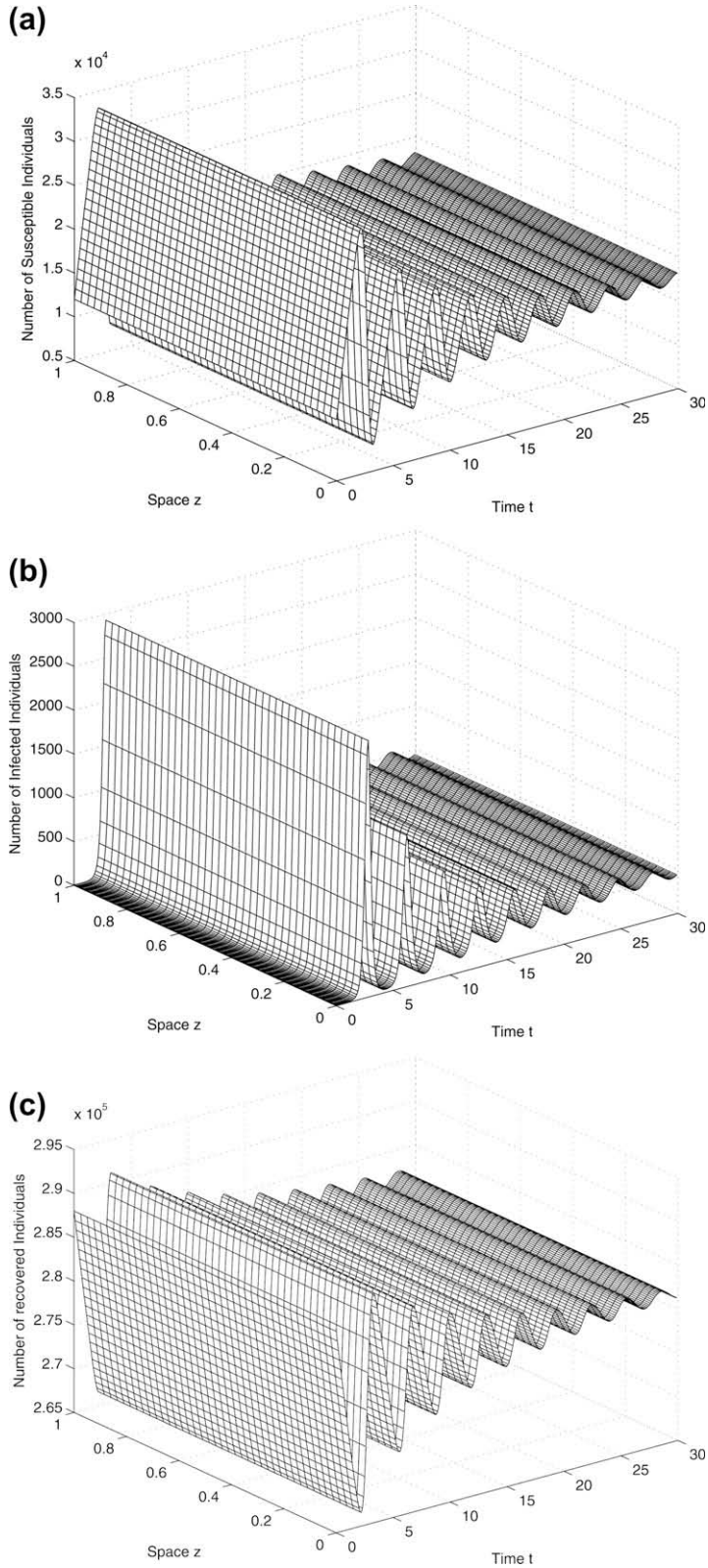

Fig. 4. Numerical simulation of the model (1.2) with $h = 0.025, \ell = 0.1$ and $r_0 = 17$: (a) profiles for susceptibles, (b) profiles for infectives and (c) profiles for recovered.

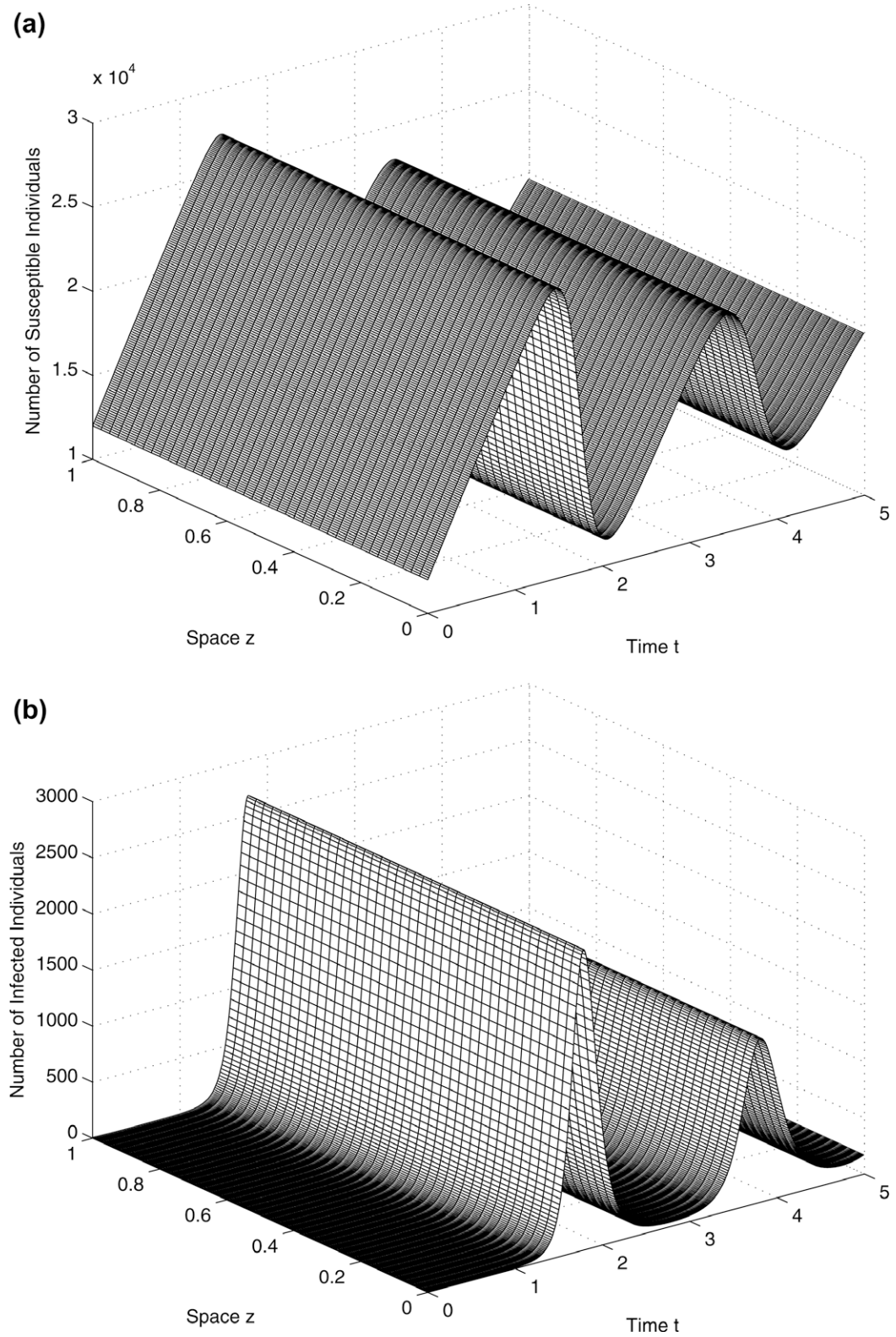

Fig. 5. Numerical simulation of the model (1.2) with $h = 0.025, \ell = 0.01$ and $r_0 = 17$: (a) profiles for susceptibles, (b) profiles for infectives.

diffusive rate were given the values $\alpha = 0.0005, 0.001, 0.01, 0.04$. The numerical results at $t = 0.1$ are depicted in Fig. 2. These show that, as time increases, the number of susceptibles are less than the number of infectious individuals until

the time $t = 0.09$ after which the number of susceptibles becomes less than the number of infectious individuals, near the middle of the interval for $\alpha = 0.0005$ and $\alpha = 0.001$ (see Fig. 2(a), (b)). As α is increased, the number of susceptibles becomes larger than the number of infectious individuals (Fig. 2(c), (d)), moreover, the number of infectious individuals spread on the z-axis. These reveal the dynamic behaviour of whooping cough depends on the diffusion rate which supported that diffusion plays a significant role in shaping the dynamical behaviour of biological system [24,4].

5.3. Experiment 3: Effect of transmissibility coefficient, β

The effectiveness of the transmissibility coefficient is monitored for studying asymptotic behaviour of an SIR epidemic model and describing the transmission of diseases such as whooping cough. We simulate the model (4.1)–(4.5) using the numerical method $DM(\theta), \theta = 1$, with the following initial conditions and parameters: $S_0 = 1200, I_0 = 7.5, \mu = 0.04, \nu = 24, \alpha = 0.4, N = 3 \times 10^5$ and varying values of β.

Let $\beta = 9.2 \times 10^{-7}$, then $r_0 = 0.9567$. It is easy to see that system (1.2) admits the disease-free equilibrium $e^0 = (3 \times 10^5, 0, 0)$. According to Theorem 3.2, the disease-free equilibrium e^0, is globally asymptotically stable, as shown in Fig. 3. It interprets that the infected humans with whooping cough appear to be pandemic initially and are eventually extinct. It suggests that to reduce the contact rate for the susceptible humans is the good policy in order to control the spread of whooping cough.

The reproductive number, r_0, of whooping cough has been documented of order 16–20 [2,31]. When $\beta = 1.4 \times 10^{-3}$, then $r_0 = 17$. It is seen that system admits an endemic equilibrium $e^+ = (17647 \times 10^4, 469, 2.8188 \times 10^5)$. According to Theorem 3.1, we get that the positive solution of system (1.2) converges to e^+ when $t \to \infty$ as shown in Fig. 4. Fig. 5 shows the numbers of susceptible and infected individuals at time $t = 5$. In Fig. 5(b), the number of infected individuals fall in the inter-epidemic period, which means that the disease was not endemic. A corresponding simulation for the number of susceptible individuals shows a progressive build up by new births during the inter-epidemic period and a dramatic fall during the epidemic see Fig. 5(a). These imply that the population takes two years to build up the pool of susceptibles to threshold size/density $(S > N_T)$ which agrees with the spatial data for whooping cough in England and Wales reported in Rohani et al. [38]. Fig. 5(b) also shows that whooping cough remains an endemic disease with epidemic outbreaks every 3 years which confirms in many parts of the world whooping cough remains an endemic disease with epidemic outbreaks every 3–5 years [6]. It interprets that the infected humans outbreak and eventually keep the relatively high level of the size if the contact rate is big. It suggests that the endemic will occur if we do not take efficient measures to control the spread of whooping cough.

6. Discussion and conclusions

In this paper, the SIR epidemic model with diffusion is studied describing the transmission of diseases such as whooping cough. We have obtained asymptotic behaviour results and numerical simulations have been presented to interpret the main results. It is observed that if $(r_0 < 1)$, the disease-free equilibrium e^0 is globally asymptotically stable, which implies that the humans are safe if the contact rate β for the susceptible individual is small. In other words, if we do not prevent the spread of whooping cough, the pandemic will occur. Though the long time behaviour our solutions appear to be space-independent, it is our hope the future investigations of our model or variations of the model will provide useful insights on the spatial effects of the epidemic problem. For example, it would be an interesting question to know how long it takes for a spatially non-homogeneous state to evolve into a roughly spatially homogeneous state. Our results also show that the dynamics of whooping cough depends on the diffusion rate and the contract rate.

A robust finite-difference scheme, $DM(\theta)$, was constructed and used to determine the solution of the model to first-order in time and second-order in space of accuracy. This method proved to be much better, in terms of numerical stability, than the standard method, $SM(\theta)$, based on the parameter values used in our simulations.

Acknowledgements

The authors would like to express our gratitude to Professor E.H. Twizell, Brunel University, UK, for his encouragement, suggestions and comments which have improved the paper. The authors would like to thank the anonymous referee for very helpful suggestions and comments which led to improvements of our original manuscript.

Appendix A

The von Neumann or Fourier series method seek the condition(s) under which small errors of the forms

$$Z^n_{x,m} := X^n_m - \widetilde{X}^n_m = e^{\gamma n l} e^{i\delta m h}, \tag{A.1}$$

and

$$Z^n_{y,m} := Y^n_m - \widetilde{Y}^n_m = e^{\psi n l} e^{i\phi m h}, \tag{A.2}$$

where γ, ψ, δ and ϕ are real, $i = \sqrt{-1}$ and $\widetilde{X}_m^n, \widetilde{Y}_m^n$ are a perturbed numerical solutions, necessary conditions for the errors not to grow as $n \to \infty$ are (see [34])

$$|e^{\gamma\ell}| \leqslant 1 + M_x\ell \quad \text{and} \quad |e^{\psi\ell}| \leqslant 1 + M_y\ell, \tag{A.3}$$

where M_x and M_y are non-negative constants independent of h, ℓ. The conditions in (A.3) make no allowance for growing solutions if $M_x = 0$ and $M_y = 0$.

Method $SM(\theta)$: Substituting Z_x into (4.18) leads to the (local) stability equation

$$\left\{1 + 4p\theta\sin^2\frac{\delta h}{2}\right\}\xi_x = 1 - 4p(1-\theta)\sin^2\frac{\delta h}{2} - \mu\ell - \ell\beta Y_m^n, \tag{A.4}$$

where $\xi_x = e^{\gamma\ell}$ and Y_m^n is treated as a (local) constant. The von Neumann necessary condition for stability is $|\xi_x| < 1$, that is, the stability restrictions are

$$\begin{aligned}
&0 \leqslant \theta < 1/2, \quad p \leqslant \frac{2 - \ell(\mu + \beta Y_m^n)}{4(1-2\theta)},\\
&\theta = 1/2, \quad \ell(\mu + \beta Y_m^n) \leqslant 2 \quad \text{and} \quad p > 0,\\
&1/2 < \theta \leqslant 1, \quad p \geqslant \frac{\ell(\mu + \beta Y_m^n) - 2}{4(2\theta - 1)}.
\end{aligned} \tag{A.5}$$

Substituting Z_y into (4.19) gives the (local) stability equation

$$\left\{1 + 4p\theta\sin^2\frac{\phi h}{2}\right\}\xi_y = 1 - 4p(1-\theta)\sin^2\frac{\phi h}{2} - (\mu + \nu)\ell + \beta\ell X_m^n, \tag{A.6}$$

where $\xi_y = e^{\psi\ell}$ and X_m^n is treated as a (local) constant. The von Neumann necessary condition for stability is $|\xi_y| < 1$, that is, the stability restrictions are

$$\begin{aligned}
&0 \leqslant \theta < 1/2, \quad p \leqslant \frac{2 + \ell\beta X_m^n - \ell(\mu + \nu)}{4(1-2\theta)} \quad \text{and} \quad p \geqslant \frac{-(\mu + \nu - \beta X_m^n)\ell}{4},\\
&\theta = 1/2, \quad 2 + \beta\ell X_m^n - (\mu + \nu)\ell \geqslant 0 \quad \text{and} \quad p \geqslant \frac{-(\mu + \nu - \beta X_m^n)\ell}{4},\\
&1/2 < \theta \leqslant 1, \quad p \geqslant \frac{-2 + \ell(\mu + \nu) - \ell\beta Y_m^n}{4(2\theta - 1)} \quad \text{and} \quad p \geqslant \frac{-(\mu + \nu - \beta X_m^n)\ell}{4}.
\end{aligned} \tag{A.7}$$

Method $DM(\theta)$: Substituting Z_x into (4.10) leads to the stability equation

$$\left\{1 + \ell\mu + \ell\beta Y_m^n + 4p\theta\sin^2\frac{\delta h}{2}\right\}\xi_x = 1 - 4p(1-\theta)\sin^2\frac{\delta h}{2}, \tag{A.8}$$

from which it may be deduced that, for stability,

$$\begin{aligned}
&0 \leqslant \theta < 1/2, \quad p \leqslant \frac{2 + \ell\mu + \ell\beta Y_m^n}{4(1-2\theta)},\\
&\theta = 1/2, \quad p > 0,\\
&1/2 < \theta \leqslant 1, \quad p > 0.
\end{aligned} \tag{A.9}$$

Substituting Z_y into (4.11) gives to the stability equation

$$\left\{1 + (\mu + \nu)\ell + 4p\theta\sin^2\frac{\phi h}{2}\right\}\xi_y = 1 - 4p(1-\theta)\sin^2\frac{\phi h}{2} + \ell\beta X_m^n, \tag{A.10}$$

with the consequent stability restrictions

$$\begin{aligned}
&0 \leqslant \theta < 1/2, \quad p \leqslant \frac{2 + (\mu + \nu)\ell + \ell\beta X_m^n}{4(1-2\theta)} \quad \text{and} \quad p \geqslant \frac{-(\mu + \nu)\ell + \ell\beta X_m^n}{4},\\
&\theta = 1/2, \quad p \geqslant \frac{-(\mu + \nu)\ell + \ell\beta X_m^n}{4},\\
&1/2 < \theta \leqslant 1, \quad p \geqslant \frac{-(\mu + \nu)\ell + \ell\beta X_m^n}{4}.
\end{aligned} \tag{A.11}$$

It is followed that the stability intervals of the method $SM(\theta)$ and $DM(\theta)$ are given by the intersection of the restriction on p in each value of θ, see Eqs. {(A.5) and (A.7)} and {(A.9) and (A.11)}, respectively. The method $DM(\theta)$ is seen to be more competitive (in terms of stability intervals) than the method $SM(\theta)$. Numerical simulations is demonstrated in Section 5.1 to confirm these results.

Appendix B

The derivative $\partial S/\partial z$ in (4.5) may be approximated by the second-order, central-difference replacement

$$\frac{\partial S(z,t)}{\partial z} = \frac{S(z+h,t) - S(z-h,t)}{2h} + O(h^2), \tag{B.1}$$

with a similar replacement being made to $\partial I/\partial z$. The implementation of the boundary conditions (4.5), yield, on $z = 0$ and $z = L$,

$$X_1^n = X_{-1}^n,\ Y_1^n = Y_{-1}^n \quad \text{and} \quad X_{M+1}^n = X_{M-1}^n,\ Y_{M+1}^n = Y_{M-1}^n\ (n = 0, 1, 2, \ldots), \tag{B.2}$$

to second-order thus introducing the exterior grid points $(z_{-1}, t) = (-h, n\ell)$ and $(z_{M+1}, t) = ((M+1)h, n\ell)$.

Let $\mathbf{X}^{n+1} = \left[X_0^{n+1}, X_1^{n+1}, \ldots, X_M^{n+1}\right]^T$ and $\mathbf{Y}^{n+1} = \left[Y_0^{n+1}, Y_1^{n+1}, \ldots, Y_M^{n+1}\right]^T$ where T denotes transpose. The modification to the formulae of the families of methods $SM(\theta)$ and $DM(\theta)$, and their implications, are as follows.

Method $SM(\theta)$:

Taking $m = 0, M$ in (4.18) and (4.19) and using (B.2) gives

$m = 0$,

$$(1+2p\theta)X_0^{n+1} - 2p\theta X_1^{n+1} = \left\{1 - \ell\mu - \ell\beta Y_0^n - 2p(1-\theta)\right\}X_0^n + 2p(1-\theta)X_1^n + \ell\mu N, \tag{B.3}$$

$$(1+2p\theta)Y_0^{n+1} - 2p\theta Y_1^{n+1} = \left\{1 - (\mu+\nu)\ell + \ell\beta X_0^n - 2p(1-\theta)\right\}Y_0^n + 2p(1-\theta)Y_1^n, \tag{B.4}$$

and $m = M$,

$$-2p\theta X_{M-1}^{n+1} + (1+2p\theta)X_M^{n+1} = -2p(1-\theta)X_{M-1}^n + \left\{1 - \ell\mu - \ell\beta Y_M^n - 2p(1-\theta)\right\}X_M^n + \ell\mu N, \tag{B.5}$$

$$-2p\theta Y_{M-1}^{n+1} + (1+2p\theta)Y_M^{n+1} = 2p(1-\theta)Y_{M-1}^n + \{1 - (\mu+\nu)\ell + \ell\beta X_M^n - 2p(1-\theta)\}Y_M^n. \tag{B.6}$$

The solution vectors $\mathbf{X}^{n+1}$ and $\mathbf{Y}^{n+1}$ may be obtained using the following parallel algorithm:

$$\textbf{Processor 1}: \text{Solve} \quad E_1\mathbf{X}^{n+1} = F_1\mathbf{X}^n + \mathbf{q} \quad \text{for} \quad \mathbf{X}^{n+1}, \tag{B.7}$$

$$\textbf{Processor 2}: \text{Solve} \quad E_1\mathbf{Y}^{n+1} = G_1\mathbf{Y}^n \quad \text{for} \quad \mathbf{Y}^{n+1}, \tag{B.8}$$

where E_1 is a constant, tridiagonal matrix of order $M+1$ and $\mathbf{q} = [\ell\mu N, \ldots, \ell\mu N]^T$, T denoting transpose, is a constant vector of order $M+1$. The square matrices $F_1 = F_1(\mathbf{Y}^n)$ and $G_1 = G_1(\mathbf{X}^n)$ are also of order $M+1$. th element of E_1, F_1, and G_1 are easily obtained from (B.3)–(B.6), (4.18) and (4.19) with $m = 1, 2, \ldots, M$.

Method $DM(\theta)$:

Taking $m = 0, M$ in (4.10) and (4.11) and using (B.2) gives

$m = 0$,

$$(1+\mu\ell+\ell\beta Y_0^n + 2p\theta)X_0^{n+1} - 2p\theta X_1^{n+1} = \{1 - 2p(1-\theta)\}X_0^n + 2p(1-\theta)X_1^n + \ell\mu N, \tag{B.9}$$

$$(1+(\mu+\nu)\ell + 2p\theta)Y_0^{n+1} - 2p\theta Y_1^{n+1} = \{1 + \ell\beta X_0^n - 2p(1-\theta)\}Y_0^n + 2p(1-\theta)Y_1^n, \tag{B.10}$$

and $m = M$,

$$-2p\theta X_{M-1}^{n+1} + (1+\mu\ell+\ell\beta Y_M^n + 2p\theta)X_M^{n+1} = 2p(1-\theta)X_{M-1}^n + \{1 - 2p(1-\theta)\}X_M^n + \ell\mu N, \tag{B.11}$$

$$-2p\theta Y_{M-1}^{n+1} + (1+(\mu+\nu)\ell + 2p\theta)Y_M^{n+1} = 2p(1-\theta)Y_{M-1}^n + \{1 + \ell\beta X_M^n - 2p(1-\theta)\}Y_M^n. \tag{B.12}$$

In this method the solution vectors $\mathbf{X}^{n+1}$ and $\mathbf{Y}^{n+1}$ may be obtained using the parallel algorithm:

$$\textbf{Processor 1}: \text{Solve} \quad O_1\mathbf{X}^{n+1} = P_1\mathbf{X}^n + \mathbf{q} \quad \text{for} \quad \mathbf{X}^{n+1}, \tag{B.13}$$

$$\textbf{Processor 2}: \text{Solve} \quad Q_1\mathbf{Y}^{n+1} = R_1\mathbf{Y}^n \quad \text{for} \quad \mathbf{Y}^{n+1}, \tag{B.14}$$

in which all matrices are square and of order $M+1$. The element of $O_1 = O_1(\mathbf{Y}^n), R_1 = R_1(\mathbf{X}^n)$, and the constant matrices P_1 and Q_1 may be obtained from (B.9)–(B.12), (4.10) and (4.11) with $m = 1, 2, \ldots, M$.

As described above, the linear algebraic systems given by {(B.7) and (B.8)} and {(B.13) and (B.14)} can be solved using parallel computation (using a computer with two processor). In parallel computation, the vectors $\mathbf{X}^{n+1}$ and $\mathbf{Y}^{n+1}$ can be obtained simultaneously and thus the time taken to solve the PDEs will be reduced significant.

References

[1] R.M. Anderson, H.C. Jackson, R.M. May, A.M. Smith, Population dynamics of foxes rabies in Europe, Nature 289 (1981) 765–771.
[2] R.M. Anderson, R.M. May, Infectious Diseases of Humans: Dynamics and Control, Oxford University Press, 1992.

[3] L.J.S. Allen, B.M. Bolker, Y. Lou, A.L. Nevai, Asymptotic profiles of the steady states for an SIS epidemic reaction–diffusion model, Discrete Contin. Dyn. Syst. A 21 (1) (2008) 1–20.
[4] R. Bhattacharyya, B. Mukhopadhyay, M. Bhattacharyya, Diffusion-driven stability analysis of a prey–predictor system with Holling type-IV functional response, Syst. Anal. Model. Smul. 43 (8) (2003) 1085–1093.
[5] F. Brauer, C. Castillo-Chavez, Mathematical Models in Population Biology and Epidemiology, Springer, New York, 2001.
[6] N.S. Crowcroft, J. Britto, Whooping cough: a continuing problem, BMJ 324 (2002) 1537–1538.
[7] S. Busenberg, P. van den Driessche, Analysis of a disease transmission model in a population with varying size, J. Math. Biol. 28 (1990) 257–270.
[8] R.S. Cantrell, C. Cosner, Spatial Ecology via reaction–diffusion Equations, Wiley, Chichester, 2003.
[9] O. Diekmann, J.A.P. Heesterbeek, Mathematical Epidemiology of Infectious Diseases, Model Building, Analysis and Interpretation, Wiley, New York, 2000.
[10] O. Diekmann, M. Kretzschmar, Patterns in the effects of infectious diseases on population growth, J. Math. Biol. 29 (1991) 539–570.
[11] C.J. Ducan, S.R. Duncan, S. Scott, Whooping cough epidemics in London, 1701–1812: infection dynamics, seasonal forcing and the effects of malnutrition, Proc. R. Soc. Lond. B 263 (1996) 445–450.
[12] N.M. Ferguson, D.J. Nokes, R.M. Anderson, Dynamical complexity in age-structured models of the transmission of measles virus, Math. Biol. 138 (1996) 101–130.
[13] L.Q. Gao, H.W. Hethcote, Disease transmission models with density-dependent demographics, J. Math. Biol. 30 (1992) 713–717.
[14] D.Z. Girard, Intervention times series analysis of pertussis vaccination in England and Wales, Health Policy 54 (2000) 13–25.
[15] B.T. Grenfell, B.M. Bolker, A. Kleczkowski, Seasonality and extinction in chaotic metapopulations, Proc. Roy. Soc. Lond. B 259 (1995) 97–103.
[16] D. Henry, Geometric Theory of Semilinear Parabolic Equations, Lecture Notes in Mathematics, vol. 840, Springer-Verlag, Berlin, New York, 1993.
[17] Q. He, M.K. Viljanem, et al, Outcomes of Bordetella pertussis infection in different age groups of an immunized population, J. Infect. Dis. 170 (1994) 873–877.
[18] M.J. Keeling, B.T. Grenfell, Disease extinction and community size: modelling the persistence of measles, Science 275 (1997) 65–67.
[19] M.J. Keeling, P. Rohani, B.T. Grenfell, Seasonally forced disease dynamics explored as switching between attractors, Physica D 148 (2001) 317–335.
[20] W.O. Kermack, A.G. McKendrick, Contribution to the mathematical theory of epidemics, part I, Bull. Math. Biol. 53 (2006) 33–55.
[21] Z.G. Lin, M. Pedersen, Stability in a diffusive food-chain model with Michaelis–Menten function response, Nonlinear Anal. 57 (2004) 421–433.
[22] J.D. Murray, Mathematical Biology II: Spatial Models and Biomedical Applications, third ed., Springer, Berlin, 2003.
[23] D. Mollison, V. Isham, B. Grenfell, Epidemics: models and data, J. Roy. Stat. Soc. A 157 (1993) 115–149.
[24] A. Okubo, Diffusion and Ecological Problems, in: Mathematical Models, Springer, New York, 1980.
[25] L.F. Olsen, G.L. truty, W.M. Schaffer, Oscillations and chaos in epidemics: a nonlinear dynamic study of six childhood diseases in Copenhagen, Denmark, Theor. Popul. Biol. 33 (1986) 344–370.
[26] P.Y.H. Pang, M.X. Wang, Strategy and stationary pattern in a three species predator–prey model, J. Diff. Eqs. 200 (2004) 245–273.
[27] W. Piyawong, Ph.D. thesis, Brunel University, England, 2001.
[28] M.H. Protter, H.F. Weinberger, Maximum Principles in Differential Equations, Prentice Hall, Englewood Cliffs, 1967.
[29] D.A. Rand, H.B. Wilson, Chaotic stochasticity – a ubiquitous source of unpredictability in epidemics, Proc. Roy. Soc. Lond. B 246 (1991) 179–184.
[30] P. Rohani, D.J.D. Eam, B.T. Grenfell, Opposite patterns of synchrony: in sympatric disease metapopulations, Science 286 (1999) 968–971.
[31] P. Rohani, D.J. Earn, B. Finkenstädt, B.T. Grenfell, Population dynamic interference among childhood diseases, Proc. Roy. Soc. Lond. B 2865 (1998) 2033–2041.
[32] W.M. Schaffer, M. Kot, Nearly one-dimensional dynamics in an epidemic, J. Theor. Biol. 112 (1985) 403–427.
[33] D. Schenzle, An age-structured model of pre- and post-vaccination measles transmission, IMA J. Math. Appl. Med. Biol. 1 (1984) 169–191.
[34] G.D. Smith, Numerical Solution of Partial Differential Equations: Finite Difference Methods, third ed., Clarendon Press, Oxford, 1985.
[35] G. Sugihara, B.T. Grenfell, R.M. May, G.L. Truty, W.M. Schaffer, Distinguishing error from chaos in ecological time series, Philos, Trans. Roy. Soc. Lond. B 330 (1990) 235–251.
[36] E.H. Twizell, Numerical Methods, With Applications in the Biomedical Sciences, Ellis Horwood, Chichester, UK, 1988.
[37] J. Zhou, H.W. Hethcote, Population size dependent incidence in models for diseases without immunity, J. Math. Biol. 32 (1994) 809–834.
[38] P. Rohani, D.J.D. Earn, B.T. Grenfell, Opposite patterns of synchrony in sympatric disease metapopulations, Science 286 (1999) 968–971.